P1.11 A SIMPLE 3-DIMENSIONAL URBAN ENERGY BALANCE MODEL AND OUTDOOR SCALE MODEL EXPERIMENTS

Toru Kawai*, Manabu Kanda and Masahiko Kanega
Tokyo Institute of Technology, Tokyo, Japan

1. INTRODUCTION

Although the urban surface geometry largely influences the upper atmosphere, conventional atmospheric models have treated the urban areas simply as a slab surface. Recently, in order to reflect the influence of urban surface geometry on atmospheric models, simple urban canopy models have been developed (Masson(2000), Kusaka et al.(2001)). However, these models assume infinite long 2-dimensional street canyons mainly because 3-dimensional radiation processes are very complex and usually time-consuming to be calculated. In this paper, a *S*imple 3-dimensional *U*rban canopy *M*odel for *M*eso-scale simulation (*SUMM*) is proposed. In the model, complex 3-dimensional radiation processes are theoretically solved, and the model can predict the energy balance at each of the constituent faces (a roof, a floor and 4 vertical walls) separately. Similar outdoor scale model experiments have been conducted to examine the unknown model parameters (i.e. turbulent transfer coefficients) and to construct databases of model validation studies.

2. URBAN CANOPY MODEL (SUMM)

2.1 *Surface Geometry*

The model geometry is illustrated in Fig.1. Each building is regularly arranged to form square horizontal cross-sections. The constituent faces (resolution of the model) are a roof, a floor and 4 vertical walls. The surface geometry is idealized by the following two geometrical parameters, (1) plane area index (λ_p) and (2) frontal area index (λ_f), each expressed by Equations (1) and (2).

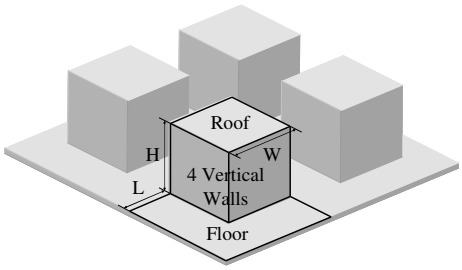

Fig.1 Urban surface geometry

* *Corresponding author address:* Toru Kawai, Tokyo Institute of Technology, Dept. of International Development Eng., Meguro-ku, O-okayama,2-12-1 Tokyo, 152-8552 JAPAN;
e-mail: kawai@ide.titech.ac.jp

$$\lambda_P = W^2/(W+L)^2 \quad (1)$$

$$\lambda_f = W \times H/(W+L)^2 . \quad (2)$$

Where, *W*, *L* and *H* are the width of the building, the width of the street and the height of the building, respectively.

2.2 *Short Wave Radiation Budget at Each Face*

In the simplified models, all faces are usually assumed to be lambertian surfaces because mirror reflection components can not be estimated without highly resolved grid spacing. Using this assumption, we can produce the following simple formulations for multi-reflections inside the street canyons. For the first reflection, absorbed ($R_{ab}(i,1)$) and reflected ($R_{ref}(i,1)$) components at face *i* are expressed by,

$$R_{ab}(i,1) = (1-a(i))R_S(i) + (1-b(i))R_{d0}(i)V(i,sky) \quad (3)$$

$$R_{ref}(i,1) = a(i)R_S(i) + b(i)R_{d0}(i)V(i,sky) . \quad (4)$$

Where, $a(i)$ is a facet albedo of direct short wave radiation at face *i*, $b(i)$ a facet albedo of diffuse short wave radiation at face *i*, $R_S(i)$ a sharing ratio of direct shortwave radiation at face *i* of a unit lot area, $R_{d0}(i)$ a diffuse shortwave radiation reaching a unit lot area of face *i*, and $V(i,sky)$ a sky view factor of face *i*, respectively. Similarly, *N*-th absorbed ($R_{ab}(i,N)$) and reflected ($R_{ref}(i,N)$) components at face *i* are,

$$R_{ab}(i,N) = (1-b(i))\sum_{j=1}^{6} R_{ref}(j,N-1)V(j,i) , \quad (5)$$

$$R_{ref}(i,N) = b(i)\sum_{j=1}^{6} R_{ref}(j,N-1)V(j,i) . \quad (6)$$

Where, $R_{ref}(i,N-1)$ is a *N-1*-th reflected component at face *i*, and $V(j,i)$ a view factor from face *j* to face *i*. A total absorption of shortwave radiation at face *i* ($RT_{ab}(i)$) after *Nmax*-th reflection is estimated as,

$$RT_{ab}(i) = \sum_{N=1}^{N\max} R_{ab}(i,N) . \quad (7)$$

In the calculation of radiation budget mentioned above, the view factors ($V(j,i)$ and $V(i,sky)$) and the sharing ratios of direct shortwave radiation ($R_S(i)$) are difficult to estimate. In this model, these two parameters are estimated theoretically. The detailed procedures for their determination are described in Kanda et al. (2004).

2.3 *Long Wave Radiation Budget at Each Face*

Since the reflected and emitted components of long wave radiation at individual faces are isotropic, the algorithm for solving the long wave radiation budget is essentially the same as that for the diffuse short wave radiation. Therefore, just as in the case of the calculation of short wave radiation budget, simple formulations for calculating the long wave radiation budget is possible as shown in the following formula. The absorbed and reflected long wave radiation per unit area of each face at the first reflection ($L_{ab}(i,1)$ and $L_{ref}(i,1)$) can be expressed by,

$$L_{ab}(i,1) = \varepsilon(i)L\downarrow V(i,\ sky) - \sigma\varepsilon(i)T_S(i)^4, \quad (8)$$

$$L_{ref}(i,1) = (1-\varepsilon(i))L\downarrow V(i,\ sky) + \sigma\varepsilon(i)T_S(i)^4. \quad (9)$$

Where $L\downarrow$ is the long wave radiation from the sky, $\varepsilon(i)$ the emissivity at face *i*, σ Stefan-Boltzmann constant, and $T_s(i)$ the surface temperature at face *i* which will be predicted in the model. The absorbed and reflected long wave radiation per unit area of face *i* at *N*-th reflection ($L_{ab}(i,N)$ and $L_{ref}(i,N)$) can be calculated by,

$$L_{ab}(i,N) = \sum_{j=1}^{6} \varepsilon(i)L_{ref}(j,N-1)V(i,j) \quad (10)$$

$$L_{ref}(i,N) = \sum_{j=1}^{6} (1-\varepsilon(i))L_{ref}(j,N-1)V(i,j). \quad (11)$$

Finally, the total absorption and reflection of long wave radiation per unit area of face *i* after $N_{\max}$ multi-reflections ($LT_{ab}(i)$ and $LT_{ref}(i)$) are calculated by,

$$LT_{ab}(i) = \sum_{N=1}^{N\max} L_{ab}(i,\ N) \quad (12)$$

$$LT_{ref}(i) = \sum_{N=1}^{N\max} L_{ref}(i,\ N). \quad (13)$$

2.4 *Sensible Heat Fluxes from Each Face*

The conventional heat transfer expression using a network of resistance (Masson(2000), Kusaka et al.(2001)) is applied for the formulation of the local sensible heat flux from the face *i* to the sky ($H(i)$)(Fig. 2),

$$H(i) = c_p \rho C_H(i) U_a (T_a - T_s(i)). \quad (14)$$

Where c_p is specific heat, ρ air density, U_a and T_a are the wind velocity and air temperature at a reference height (z_a), respectively. $C_H(i)$ is the bulk transfer coefficient. By relating the network resistance expression to the slab-type formulation (Fig. 2), the sensible heat flux (H) from overall urban surface which is calculated by continuity equation of local sensible heat fluxes can be written as,

$$H = c_p \rho C_H U_a (T_a - TH). \quad (15)$$

Where C_H and TH are the bulk transfer coefficient and aerodynamic temperature. In the determination of bulk transfer coefficients, we adopt the following two-step approach. First, C_H is theoretically predicted using the Monin-Obukhov's Similarity Theory,

$$C_H = \frac{\kappa^2}{\left(\int_{Z_{0T}/L}^{(Z_a - Z_d)/L} \Phi_H(\varsigma) \frac{d\varsigma}{\varsigma} \right)^2}. \quad (16)$$

Where κ is a Karman constant, L a Monin-Obukhov length scale ζ a non dimensional height ($= z - z_d$), $\Phi_H(\zeta)$ a universal function for heat and z_0 , z_{0T} , z_d and z_a , are the roughness lengths for momentum and heat, displacement height, and a reference height, respectively. The roughness parameters z_0 and z_d can be semi-theoretically predicted from the geometric parameters (λ_p and λ_f) by using the Macdonald's formulation (1998). z_{0T} can be determined from z_0 if the ratio z_0 / z_{0T} is known.

Second, C_H is distributed to $C_H(i)$, provided that the relative values of $C_H(i)$ normalized by $C_H(i=6;roof)$ is known from the available data-set even though they are very limited. To reinforce the poor data-set of relative values of $C_H(i)$, a new methodology to measure local bulk transfer coefficient using outdoor scale model experiments is proposed in Section 3.

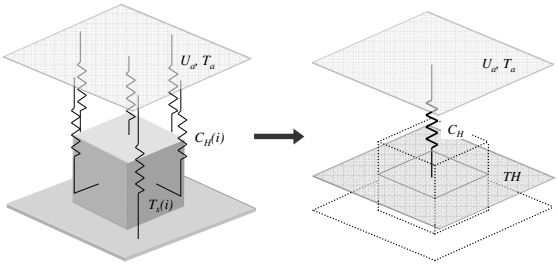

Fig.2 Resistant network expression for sensible heat transfers

2.5 *Surface Temperatures at Each Face*

Ignoring the latent heat flux contribution, the following energy balance equation holds for each face,

$$RT_{ab}(i) + RL_{ab}(i) - H(i) - LE(i) = G(i). \quad (17)$$

Where $G(i)$ is the conductive heat flux into the solids. The temperature profiles inside the walls, floor and roof are solved using one-dimensional energy conservation equation with a variable grid interval,

$$\frac{\partial T_{in}(i)}{\partial z} = \frac{1}{\rho(i)c(i)} \left(\lambda(i) \frac{\partial^2 T_{in}(i)}{\partial z^2} \right). \quad (18)$$

Where $\lambda(i)$ and $c(i)$ are the thermal conductivity and specific heat of the solid material. Equation (17) is applied as a surface boundary condition of Equation (18), and the temperature inside the solid is used as another side of the boundary condition.

3. OUTDOOR SCALE MODEL EXPERIMENTS

3.1 *Model Setup*

For the validation of the numerical model, outdoor experiments using 1/50 hardware scale models have been conducted. The site was located in Matsusaka, Mie, Japan (34º50'N, 136º50'E). The model is consisted of 0.15m cubic concrete blocks regularly distributed on flat concrete plates with a total area of 12 x 9 m^2 (Fig.3). The plane area index of the model was $\lambda_P = 0.25$. The long axis is roughly parallel to the dominant wind direction at the site (WNW). To capture an adequate developed internal boundary layer, all sensors were installed at about 10m downstream from the fetch. The up and downward short wave and long wave radiations are measured separately using a radiation-balance meter (Eiko MR-40) at 0.55m above the canopy top. To measure mean wind velocity, a compact sonic anemometer (Kaijo-WA590) with 0.05 m sensor length was installed at 0.25m above the canopy top. The conductive heat fluxes from the urban surface into the ground are measured by using very thin and highly-accurate heat plates (Captec HF-300 with 0.4-mm thickness) which are carefully coated by the same material as that of the obstacles. The surface temperatures were measured at multiple points of the faces using 0.2mm thermocouples. The air temperature was measured at the same height of sonic anemometer using 0.05mm thermocouple. All the data selected for the current analysis were under dry conditions enough to ignore the latent heat flux contribution.

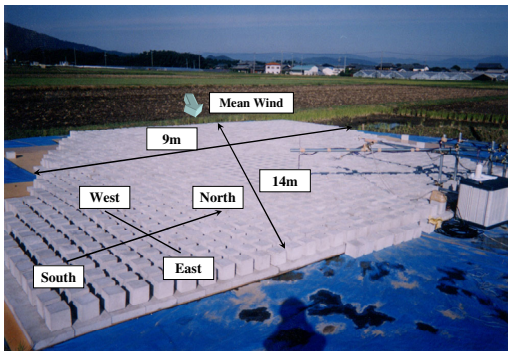

Fig.3 Outdoor scale model experiments

3.2 *Heat Transfer Coefficients*

Ignoring the latent heat contribution, the local sensible heat flux from face *i* to the sky can be expressed by,

$$H(i) = RT_{ab}(i) + RL_{ab}(i) + G(i)\,. \qquad (19)$$

In Equation (19) the net radiation component ($RT_{ab}(i) + RL_{ab}(i)$) is calculated by highly-accurate radiation scheme (kanda et al.(2004)), and the heat fluxes into the solid ($G(i)$) are measured directly from observations. Once the sensible heat flux from face *i* is determined, the bulk transfer coefficients of face *i* are calculated by Equation (14). Since the night time in the current experimental site is always windy with constant WNW wind-direction and gives almost near neutral-condition, only the nocturnal dataset is used for the ensemble average of $C_H(i)$. The atmospheric stability during the day time largely scatter and thus the limited dataset can not guarantee the statistical reliance of the estimated $C_H(i)$. Consequently, in this study, we discuss the value of $C_H(i)$ only for neutral conditions. The estimated $C_H(i)$ is compared with the indoor experiments by Narita (2003) and the present results agree well with indoor experiments (Fig.4). In Fig.4 windward walls are the north and west walls and leeward walls are the east and south walls in the current experiments.

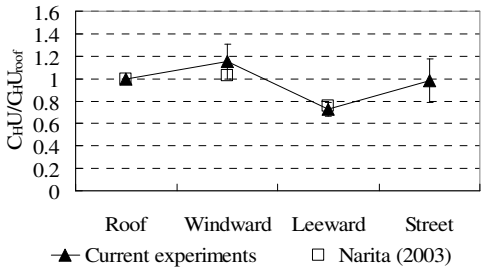

Fig.4 Estimated bulk transfer coefficients normalized by the value of the roof

4. SIMULATION RESULTS AND DISCUSSION

Except for the radiation processes, the requirement for similarity between the reduced scale model and the real world is not always met so that any quantitative discussion of surface energy balance is not always meaningful. However, once the model is evaluated by the scale model experiments, we can apply the model to the real world by adjusting the model parameters (i.e. heat capacity, thermal conductivity facet albedo, emissivity etc.). In the followings, we evaluate the simulation results of *SUMM* concerning the energy balance, surface temperatures of individual faces and overall canopy layer.

Fig.5 shows a result of simulation of net radiation at individual faces. Solid lines are the simulation results of *SUMM* and dotted lines are the simulation results derived from a highly-accurate radiation scheme (Kanda et al. (2004)). Comprehensively, the differences between the simulation results of these two models are small. However, in situations where distinguished

deviations of sunlit/shaded areas and/or of surface temperatures occur (e.g. east wall in the morning and west wall in the afternoon), the differences between these two model outputs become relatively large.

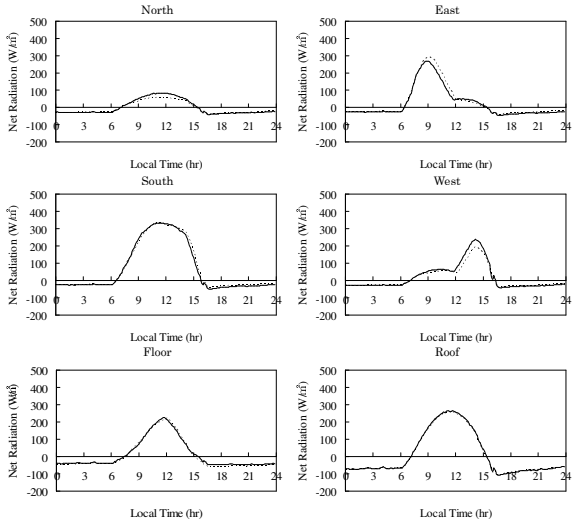

Fig.5 Net radiation at each face

Figs.6, 7 and 8 show the simulation results of ground heat flux, sensible heat flux and surface temperatures of individual faces. The solid lines are the simulation results of *SUMM* and the dotted lines show measured ground heat flux, sensible heat flux calculated by subtracting the measured ground heat flux from net radiation flux which is calculated by highly-accurate radiation scheme, and measured surface temperature, respectively. In each figure, *SUMM* well reproduces diurnal trend of changes. However, we can see partly quantitative disagreements between the solid and dotted lines, especially in daytime validations. In the current studies, the bulk transfer coefficients are derived from datasets at nighttime in which the situations are of nearly neutral stratifications, and thus the current values of local bulk transfer coefficients have been derived without consideration of the local atmospheric stabilities. As a result, while the simulation results of *SUMM* show fairly good agreement with observed values in several hours before sunrise, but in daytime and during several hours after sunset in which the daytime hysteresis of surface temperatures remain, the simulation results show relatively large disagreement with measured values.

Fig.9 shows simulation results of energy balance of whole canopy layer. Solid lines are the simulation results of *SUMM*, and dotted lines are the net radiation component simulated by a highly-accurate radiation scheme, measured ground heat flux and the sensible heat flux derived in the same way as used for the calculations of individual faces, respectively. In this simulation,

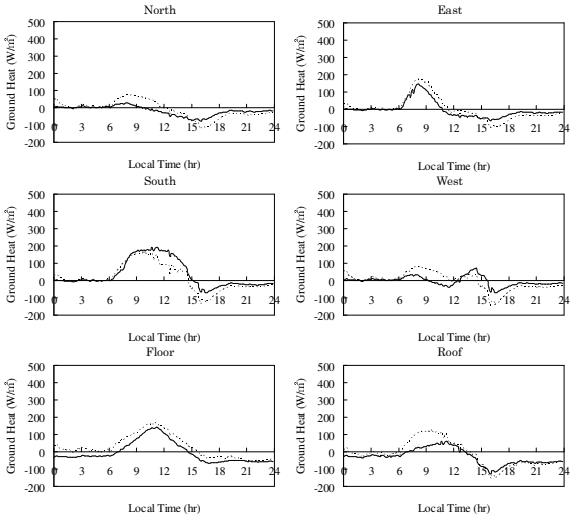

Fig.6 Ground heat flux of each face

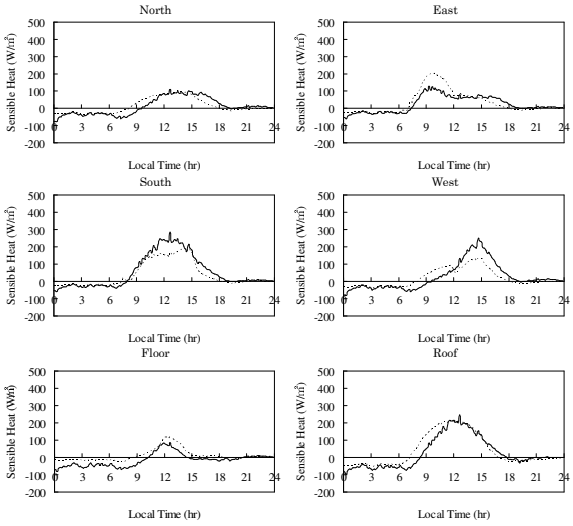

Fig.7 Sensible heat flux from each face

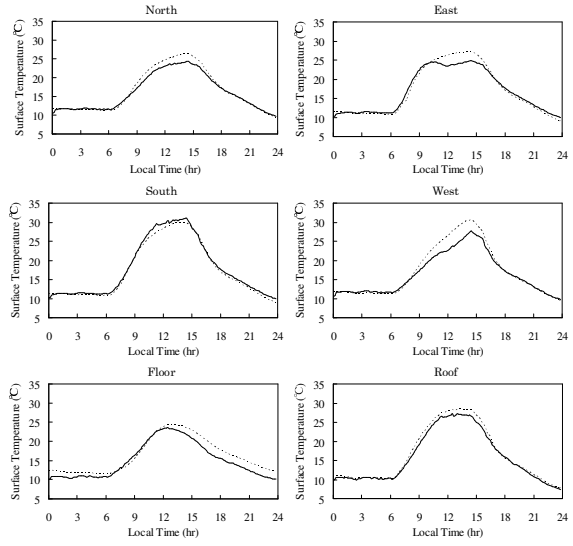

Fig.8 Surface temperatures of each face

while the net radiation component is simulated well, the simulated sensible heat flux systematically underestimates the measured value during the morning hours, which leads to the over estimation of simulated ground heat fluxes against measured value during the same period. This suggests that in situations where the local heating begins and the difference of surface temperatures among individual faces is relatively large; the value of bulk transfer coefficient of whole canopy layer becomes large compared to morning hours, which leads to the over estimation of simulated ground heat fluxes against measured value during the same period. the estimated value, in the current reduced scale model experiments.

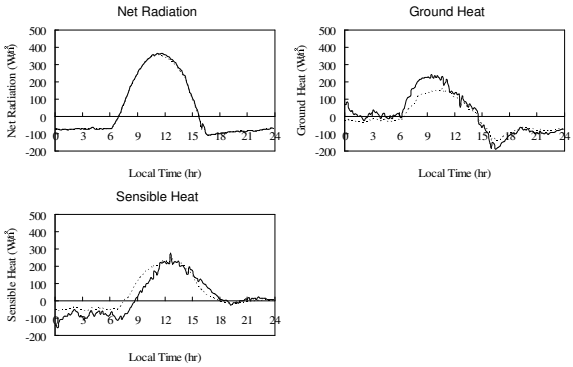

Fig.9 Energy balance components of the whole canopy layer

5. CONCULUDING REMARKS

A 3-dimensional *s*imple *u*rban energy balance *m*odel for *m*eso-scale simulations (*SUMM*) is proposed and is compared with outdoor scale-model experiments. The following major results have been obtained:

(1) The local transfer coefficients for heat of the individual surfaces under neutrally-stratified conditions were estimated using the outdoor experiments. The estimated local transfer coefficients normalized by the value of roof agreed well with those obtained from previous indoor experiments.

(2) The *SUMM* generally followed the observed diurnal trend of energy balance components of the individual surfaces, although the simulated sensible heat fluxes and ground heat fluxes partly showed the quantitative differences from the measured values. This is because the current transfer coefficients were derived from nearly neutrally -stratified conditions. This suggests the necessity for considering the influence of local atmospheric stability on the transfer coefficients.

(3) The *SUMM* simulated fairly well the observed energy balance of the whole canopy layer, although there were systematical differences between simulated results and measured values during the morning hours as to ground heat flux and sensible heat flux.

ACKNOWLEDGEMENTS

This research was financially supported by Core Research for Evolution Science and Technology of the Japan Science and Technology Cooperation, and by a Grant-in-Aid for Developmental Scientific Research from the Ministry of Education, Science and Culture of Japan.

REFERENCE

Arnfield, A. J., 1982: An Approach to the Estimation of the Surface Radiative Properties and Radiation Budgets of Cities. *Phys. Geogr.*, **3**, 97-122.

Barlow, J. F. and Belcher, S.E., 2002: A Wind Tunnel Model for Quantifying Fluxes in The Urban Boundary Layer. *Boundary-Layer Meteorol.*, **104**, 131-150.

Barlow, J. F., Harman I. N. and Belcher S. E, 2004: Scalar Fluxes from Urban Street Canyons. Part 1: Laboratory Simulation. *Boundary-Layer Meteorol.* (in print).

Hagishima, A., Tanimoto, J. and Narita, K., 2004: Review of Experimental Research on the Convective Heat Transfer Coefficient of Urban Surfaces. *Boundary-Layer Meteorol.* (submitted)

Kanda, M., 2004: Progress in The Scale Modeling of Urban Climate: Review. *Theor. Appl. Climatol.* (accepted).

Kanda, M. and Moriwaki, R, 2002: Surface Parameters in a Densely Built-up Residential Area in Tokyo. *Proc. 4th Sympo. Urban Environ.*, 147-148.

Kanda, M., Kawai, T. and Nakagawa, K, 2004a: Simple Theoretical Radiation Scheme for Regular Building Array. *Boundary-Layer Meteorol.* (in press)

Kanda, M., Moriwaki, R. and Kasamatsu, F, 2004b: Large Eddy Simulation of Turbulent Organized Structure within and above Explicitly Resolved Cube Arrays. *Boundary-Layer Meteorol.* **112**, 343-368.

Kusaka, H., Kondo, H., Kikegawa, Y., and Kimura, F., 2001: A Simple Single-layer Urban Canopy Model for Atmospheric Models: Comparison with Multi-layer and Slab Models. *Boundary-Layer Meteorol.* **101**, 329-358.

Macdonald, R.W., Griffiths, R.F., and Hall, D.J., 1998: An Improved Method for the Estimation of Surface Roughness of Obstacle Arrays. *Atmos. Environ.* **32**, 1857-1864.

Martilli, A., Clappier, A. and Rotach, M.W., 2002: An Urban Surface Exchange Parameterization for Mesoscale Models. *Boundary-Layer Meteorol.* **104**, 261-304.

Masson, V., 2000: A Physically-based Scheme for the Urban Energy Budget in Atmospheric Models. *Boundary-Layer Meteorol.* **94**, 357-397.

Moriwaki, R. and Kanda, M, 2003: Radiation, Heat, Water-vapor and CO_2 Fluxes in an Urban Surface Layer. J. Japan Soc. Hydrol. and Water Resour. **16**, 477-490 (in Japanese).

Narita, K., 2003: Wind Tunnel Experiment on Convective Transfer Coefficient in Urban Street Canyon. *5th Int Conf Urban Climate* Lots Poland, O21.2 (CD-ROM).

Sailor, D. and Fan, H, 2002: Modeling the Diurnal Variability of Effective Albedo for Cities. *Atmos. Environ*. **36**, 713-725.

Swaid, H., 1993: The Role of Radiative-convective Interaction in Creating The Microclimate of Urban Street Canyons. *Boundary-Layer Meteorol*. **64**, 231-259.

Uehara, K., Wakamatsu, S. and Ooka, R., 2003: Studies on Critical Reynolds Number Indices for Wind-tunnel Experiments on Flow within Urban Areas. *Boundary-Layer Meteorol.* **107**, 353-370.

Voogt, J. A. and Oke, T. R., 1990: Validation of an Urban Canyon Radiation Model for Nocturnal Long-wave Fluxes. *Boundary-Layer Meteorol.* **54**, 347-361.

Voogt, J. A. and Grimmond, C. S. B., 2000: Modeling Surface Sensible Heat Flux using Surface Radiative Temperatures in a Simple Urban Area. *J. Appl. Meteorol.* **39**, 1679-1699.